Structure determination of the capsular polysaccharide from *Vibrio vulnificus* strain 6353

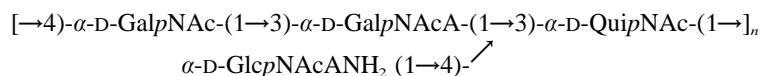G. Prabhakar REDDY[1], Unaiza HAYAT[2], Qiuwei XU[1], K. Vasavi REDDY[1], Yuhui WANG[1], Kou-Wei CHIU[1], J. Glenn MORRIS Jr[2] and C. Allen BUSH[1]

[1] Department of Chemistry and Biochemistry, University of Maryland Baltimore County, Baltimore MD, USA
[2] Departments of Medicine and Pathology, University of Maryland School of Medicine and Veterans Affairs Medical Center, Baltimore MD, USA

Vibrio vulnificus is a pathogenic gram-negative bacterium, endemic to brackish waters, which is often isolated from sediments, from the water column or from shellfish. It is associated with wound infections and septicemia in humans and the virulence of *V. vulnificus* has been strongly associated with encapsulation. The capsular polysaccharide purified from a virulent strain of *V. vulnificus* 6353 did not show cross reactivity with antibodies to the capsular polysaccharide of a related pathogenic strain of *V. vulnificus* (MO6-24) the structure of which was recently reported. NMR spectroscopic analysis of the purified polysaccharide from strain 6353 showed that the polymer is composed of four sugar residues per repeating subunit including 2,6-dideoxy-2-*N*-acetylamino-α-D-glucose (QuiNAc), 2-deoxy-2-*N*-acetylamino-α-D-galactose (α-D-GalNAc), 2-deoxy-2-*N*-acetylamino-α-D-galcturonic acid (α-D-GalNAcA) and 2-*N*-acetylamino-α-D-glucuronamide (α-D-GlcNAcANH$_2$). The ^{1}H- and ^{13}C-NMR spectra were completely assigned by homonuclear and heteronuclear NMR spectroscopy. Sugar types and anomeric configurations were determined from proton homonuclear coupling constants and glycosidic linkages were determined from ^{1}H−^{13}C heteronuclear multiple bond correlation spectra. Sugar identities were confirmed by high performance anion-exchange chromatography and absolute configurations were determined by gas chromatography in combination with molecular modeling and NMR spectroscopy. The structure of the polysaccharide repeating unit is:

$$[\rightarrow4)\text{-}\alpha\text{-D-Gal}p\text{NAc-}(1\rightarrow3)\text{-}\alpha\text{-D-Gal}p\text{NAcA-}(1\rightarrow3)\text{-}\alpha\text{-D-Qui}p\text{NAc-}(1\rightarrow]_n$$

$$\alpha\text{-D-Glc}p\text{NAcANH}_2\ (1\rightarrow4)\text{-}\nearrow$$

While there are some common features shared among the structures of the capsular polysaccharides of pathogenic strains of *V. vulnificus*, there are distinct differences in the detailed structures.

Keywords: bacteria; polysaccharide; structure; *Vibrio*; NMR.

Vibrio vulnificus is a gram-negative halophilic bacterium that is capable of causing severe wound infections and septicemia in humans [1, 2]. While wound infections can occur in healthy individuals, septicemia primarily affects compromised hosts with underlying conditions such as hemachromatosis, cirrhosis, and alcoholism. Over 50% of persons with septicemia die, and the mortality rate among patients who are hypotensive within 24 h of hospital admission exceeds 90% [3]. The organism is common in the estuarine environment [4, 5]. Infection generally develops following ingestion of raw oysters or other shellfish or exposure of a skin break to sea water containing the bacterium [2].

Correspondence to C. A. Bush, Department of Chemistry and Biochemistry, University of Maryland Baltimore County, Baltimore, MD 21250, USA

Fax: +1 410 455 2608.

E-mail: bush@umbc.edu

Abbreviations. Qui, quinovose, 6-deoxyglucose; 2D, two-dimensional; HMBC, heteronuclear multiple bond correlation; HPAEC, high-performance anion-exchange chromatography; DQF, double-quantum filtered; HMQC, heteronuclear quantum coherence; LRHMQC, long-range heteronuclear quantum coherence; HOHAHA, homonuclear Hartmann-Hahn.

V. vulnificus produces a capsular polysaccharide which is essential for virulence [6]. This capsule provides the bacterium with resistance to serum bactericidal activity and phagocytosis. The capsular material has also been shown to directly stimulate the release of tumor necrosis factor α and other cytokines from peripheral blood mononuclear cells [7]. Capsular polysaccharide-protein conjugate vaccines provide protection against lethal infection in mouse models. Antibodies raised to the purified capsular material are also protective against strains of the homologous capsular type [8, 9]. These observations underscore the need to carefully catalog *V. vulnificus* capsular types, both for studies of the role of the capsular material in pathogenesis and in exploring development of antisera for possible therapeutic use. We have presented chromatographic evidence that there is a great diversity of capsular types among different environmental and clinical isolates of *V. vulnificus* [10, 11].

We previously reported the complete chemical structure of the capsular polysaccharides from *V. vulnificus* strain MO6-24 [12] and strain B062316 [13], both virulent clinical isolates. In the present paper we describe the purification and complete structure determination of the capsular polysaccharide from strain 6353 of *V. vulnificus*. Although it has some structural simi-

larities with the capsules of strains previously reported, there are some distinct differences in the structure and stereochemistry.

MATERIALS AND METHODS

Materials. 1-Ethyl-3-(3-dimethylaminopropyl)carbodiimide and benzyl N-carbobenzoxy-α-D-glucosaminide were purchased from Sigma Chemical Co. Palladium catalyst and PtO$_2$ were purchased from Aldrich Chemical Co. 50% (by mass) NaOH was purchased from Fisher Scientific Co.

Polysaccharide isolation. Bacterial isolates retrieved from frozen stocks were grown on Luria-agar plates overnight at 30°C. Bacteria from single colonies were suspended in Luria broth and incubated overnight at 30°C. 1 ml broth culture was spread on Luria-agar in pans (28×48 cm) and incubated overnight at 30°C. Cells from two pans were harvested and suspended in 80 ml Dulbecco phosphate-buffered saline. Bacteria were shaken at 200 rpm on a rotary shaker in 250-ml baffled polystyrene bottles for 30 min at room temperature. Cells and debris were removed by centrifugation (16000×g, 20 min, 4°C), and supernatants were dialyzed with multiple changes of distilled water and concentrated about twofold by ultrafiltration (10 kDa nominal molecular mass stirred cell; Amicon). The retentates were ultracentrifuged (154000×g, 16 h, 20°C), and the supernatants were removed and subjected to enzymatic digestion with RNase A (100 μg/ml), DNase I (50 μg/ml plus 1 mM MgCl$_2$), pronase (250 μg/ml). This product was extracted sequentially with phenol and chloroform twice and the aqueous layer was dialyzed against water and the resultant sample was freeze dried [12, 13].

15 mg of this crude polysaccharide sample was passed through a Dowex 50W-X8 (H$^+$ form, 20×0.5 cm) column eluted with water and the fractions containing polysaccharide, which were not retained, were monitored by on-line absorbance at 205 nm. The absorbing fractions were pooled and freeze dried, then dissolved in deionized water and incubated at 80°C for 10 h. The sample was passed through a BioGel-P6 column (100X2 cm) using water elution and the fractions containing polysaccharide at the void volume were collected and freeze dried (≈11 mg). This sample was used for all the NMR and HPLC experiments.

Polysaccharide analysis. For carbohydrate analysis, approximately 200 μg polysaccharide was taken in a screw cap tube (13×100 mm) and 200 μl 4 M HCl was added. After hydrolysis in a heating block at 100°C for 2 h, the tube was cooled and the acid was removed by evaporating with nitrogen gas. The residue was dissolved in 200 μl water, and 20 μl was used for each HPLC injection. The hydrolysate was analyzed by HPAEC (high-performance anion-exchange chromatography) with a pulsed amperometric detector, using a Dionex BioLC gradient pump. A CarboPac PA1 (4×250 mm) pellicular anion-exchange column was used at a flow rate of 1 ml/min at room temperature. Eluant 1 was 15 mM NaOH and eluant 2 was 100 mM NaOH plus 150 mM NaOAc, prepared by suitable dilution of 50% NaOH solution with high-purity water. An IBM PC interfaced with Dionex AI-450 software was used for data collection and handling. In this analysis, useful retention times for neutral monosaccharides and amino sugars were provided by eluant 1 and eluant 2 was effective in analysis for acidic sugars.

For determination of sugar absolute configuration, the polysaccharide sample was subjected to acidic solvolysis with both (S)- and (R)-2-butanol in 4 M HCl for 24 h at 80°C. Samples were dried under N$_2$ gas flow and derivatized with trimethylsilyl chloride, hexamethyldisilazane in pyridine and analyzed by GC on an SE-30 column with a temperature program of 140−260°C

at 3°C/min [14]. Authentic standards were from a sample of *V. vulnificus* MO6/24 polysaccharide [12] which contains N-acetyl-D-galacturonic acid (D-GalNAcA) and N-acetyl-6-deoxy-L-glucosamine (L-QuiNAc).

The *V. vulnificus* 6353 polysaccharide was treated under reducing conditions intended to reduce uronic acid. Polysaccharide (6 mg) was added to 95 mg 1-ethyl-3-(3-dimethylaminopropyl)-carbodiimide in 8 ml water and the pH was maintained at 4.75 with 0.1 M HCl for 3 h. After adding a drop of octanol, 2 M NaBH$_4$ (15 ml) was added and the pH was maintained at 7.0 by adding 4 M HCl for 4 h at room temperature. Excess NaBH$_4$ was decomposed with acetic acid and the sample was passed through a Bio-Gel P2 column. The void volume was collected and freeze dried and the product (3 mg) studied by carbohydrate analysis by HPAEC-PAD as described above.

Synthesis of 2-amino-2-deoxy-D-glucuronic acid. Following the method of Heyns and Paulsen [15], benzyl N-carbobenzoxy-D-α-glucosaminide in water was oxidized using Pt catalyst at 95°C with O$_2$. Deblocking of the product by hydrogenation over Pd on charcoal was monitored at intervals by drawing aliquots and testing with HPAEC using eluant 2, (100 mM NaOH + 150 mM NaOAc). Under these chromatographic conditions the starting material eluted at approximately 4.5 min and no other peaks were observed in the chromatogram. After 3 h, the reaction was virtually complete as the peak at 4.5 min was replaced by one with a retention time of 7.6 min. The filtered product was lyophilized and exchanged twice with D$_2$O and was studied by ^{1}H-NMR, double-quantum-filtered (DQF) COSY and heteronuclear multiple quantum coherence (HMQC) spectra at 25°C.

Spectroscopy. For NMR spectroscopy, the polysaccharide sample (10 mg) was dissolved in 450 μl 99.96 % D$_2$O (Merck Sharp and Dohme Co.) after being lyophilized three times against 99.9% D$_2$O. Polysaccharide NMR spectra were recorded at 50°C and 75°C in a 5-mm RPT probe on a GN-500 spectrometer. The observed ^{1}H and ^{13}C chemical shifts are referenced with internal acetone (^{1}H and ^{13}C signals of acetone methyl group are 2.225 and 31.07 ppm down field from sodium 4,4-dimethyl-4-silapentane-1-sulfonate respectively). Two-dimensional (2D) spectra were recorded without sample spinning. Data in phase-sensitive mode were acquired using the method of States et al. [16]. DQF-COSY, HOHAHA, and NOESY were recorded at 500 MHz with standard pulse sequences at 50°C [17]. The mixing time for NOESY was 60 ms and the isotropic mixing time in HOHAHA was 72 ms. The HMQC spectrum [18] was recorded with proton detection at 50°C. Waltz-16 [19] decoupling was applied on the ^{13}C channel during acquisition. A heteronuclear multiple bond correlation spectrum (HMBC) was recorded in phase-sensitive mode [20] at 75°C. A carbonyl-selective long range-HMQC (LRHMQC) was based on HMQC with the ^{13}C carrier frequency in the carbonyl region and the 90° pulse set at 400 μs so that only the carbonyl ^{13}C magnetization was excited. The delay time was long enough (50 ms) to develop long range ^{1}H−^{13}C multiple quantum correlation and the second delay time was eliminated so that the heteronuclear antiphase magnetization developing from the first delay time did not refocus.

For detection of exchangeable amide proton signals, the *V. vulnificus* 6353 sample was dissolved in 80% H$_2$O/20% D$_2$O at pH 3.5. Water signals were suppressed with a Dante sequence [21] during the preparation and mixing periods of 2D NOESY and 2D HOHAHA experiments. A probe temperature of 40°C was selected for these experiments as a reasonable compromise for which the data could still be compared with other spectra at 50°C. At higher temperatures, the amide proton exchange rate rises, increasing the line width of amide proton signals, and at
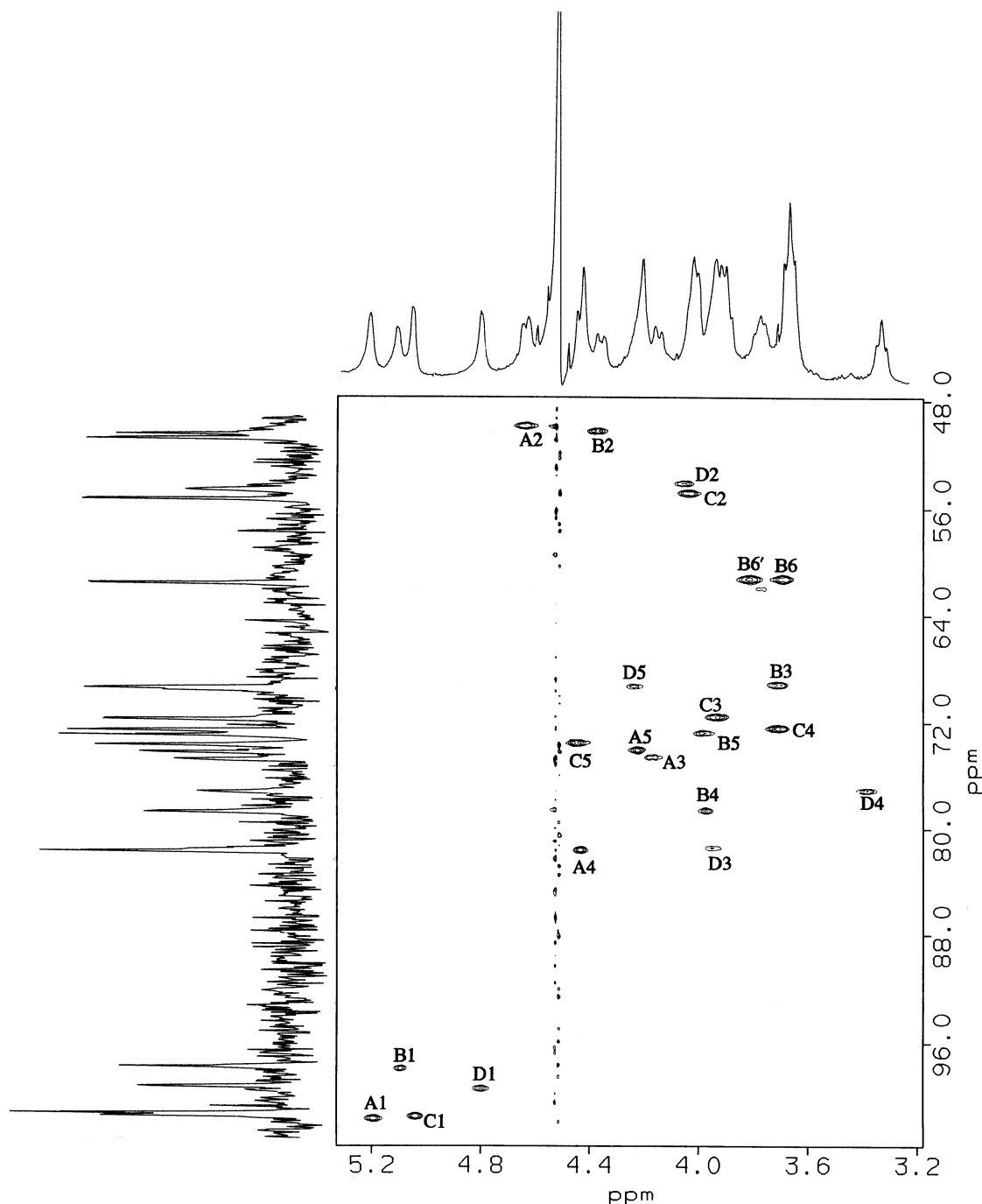
Fig. 1. Phase-sensitive ^{13}C-decoupled ^{1}H-detected HMQC spectrum of the polysaccharide from *V. vulnificus* 6353 at 500 MHz.

lower temperatures all the NMR lines broaden for reasons of polysaccharide dynamics.

Data from the GN-500 were transferred via ethernet to a VAX station 3200 or a Silicon Graphics IRIS workstation and reformatted with program GENET. NMR data processing was carried out using the Fourier-transform NMR program or Felix 2.30 (Biosym).

Molecular modeling. The polysaccharide was modeled with CHARMm version 22 (Polygen). The force field parameters were those of Polygen which are based on CHARMm parameters as modified for carbohydrates by Ha et al. [22]. The residue topology file was modified to include *N*-acetylquinovosamine and the uronic acids related to *N*-acetylglucosamine and *N*-acetylgalactosamine in both the D and L configuration. The non-

bonded interaction energy was calculated with a distance-dependent dielectric constant and a smooth-switch function with a cut-off distance of 15.0 Å. The conformations were visually checked with the QUANTA molecular graphics software (MSI-Biosym).

Disaccharides in the repeating subunit of the polysaccharide were constructed assuming the same (D) absolute configuration for both residues and also with opposite configurations, D and L. Energy maps were constructed for the glycosidic dihedral angles Φ and Ψ at 5° intervals and energy minimized. Low-energy conformations in the map were then minimized without constraints using 300 steps of steepest descent followed by 200 steps of conjugate gradient minimization and 300 steps of adapted basis Newton-Raphson. The complete tetrasaccharide repeating subunit was constructed from minimum-energy con-
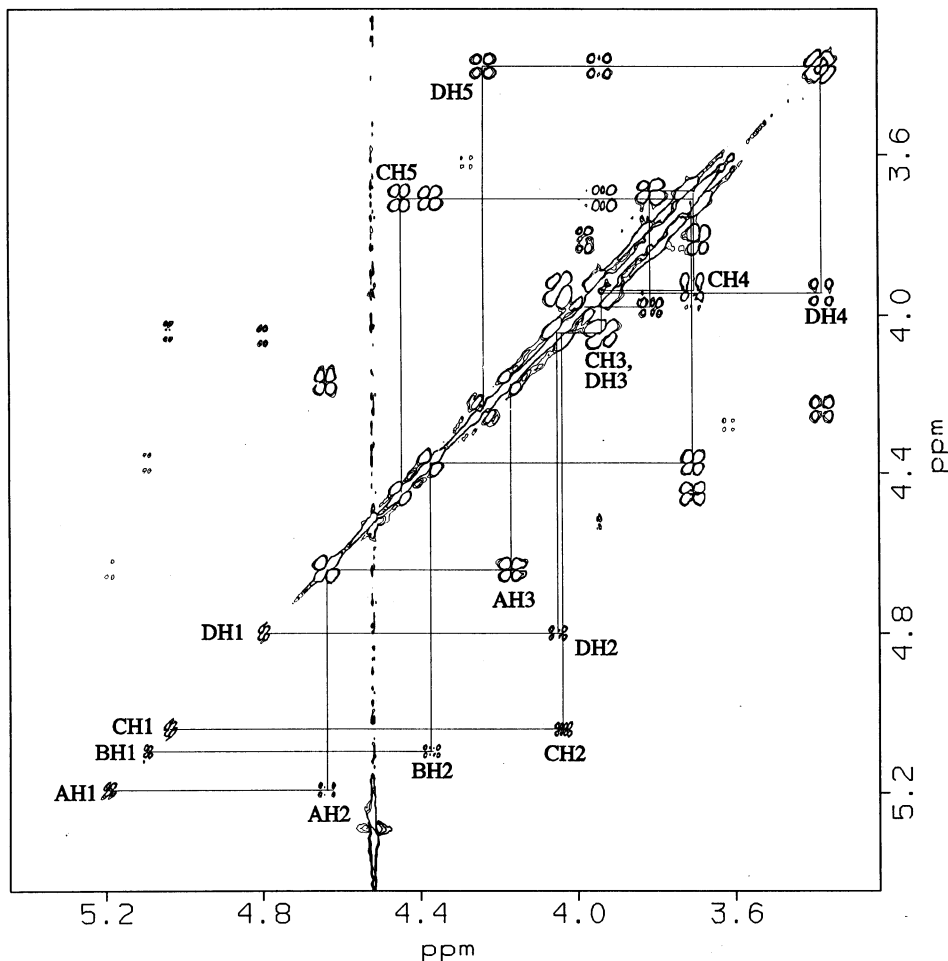
Fig. 2. Phase-sensitive DQF-COSY spectrum of the polysaccharide from *V. vulnificus* 6353 at 500 MHz.

formations of each disaccharide followed by unconstrained minimization of the tetrasaccharide. Only a small change was observed on minimization.

RESULTS

The 500-MHz ¹H-NMR spectrum of the *V. vulnificus* 6353 capsular polysaccharide, prepared without treatment with Dowex 50W (H⁺) and subsequent heating, showed fairly broad lines lacking resolved multiplets due to homonuclear coupling. The procedure described in Materials and Methods yielded a polysaccharide sample the ¹H spectrum of which, while qualitatively similar, showed improved resolution apparently because of partial hydrolysis of glycosidic linkages. ¹H NMR (Fig. 1) of the polysaccharide at 50°C shows a simple spectrum with approximately 3 Hz line width which indicates a polysaccharide having a repeating structure. A portion of the spectrum not shown in Fig. 1 contains one upfield doublet at 1.23 ppm characteristic of a methyl group of 6-deoxy sugar and resonances at 2.12 and 2.04 ppm along with one twice as intense at 2.03 ppm which suggest four methyl groups of the *N*-acetyl function in acetamido sugars. The proton resonances at 5.19, 5.09, 5.04 and 4.80 ppm show correlations to directly bonded carbon resonances in the chemical shift range 100−90 ppm characteristic for the anomeric carbon atoms of sugar residues in the ¹H-detected ¹³C-¹H single bond correlation spectrum, HMQC (Fig. 1), indicating the presence of four sugar residues in the repeating unit. The HMQC spectrum contains four resonances appearing

in the range 55−48 ppm which are characteristic of carbon bound to nitrogen which is consistent with the presence of four acetamido groups in the repeating structure.

For the purposes of ¹H and ¹³C assignment, we assign boldface letters (**A**−**D**) to each of the four residues. Starting from each anomeric proton, ¹H spin systems in each sugar residue can be assigned from 2D ¹H homonuclear spectra. The anomeric resonance at 5.19 ppm, for residue **A**, gives a cross peak to H2 at 4.64 ppm, which in turn gives a cross peak to H3 at 4.16 ppm in DQF-COSY (Fig. 2). HOHAHA shows the same connectivity (data not shown) and HMQC was used to derive the corresponding ¹³C assignments. A careful examination of H1/H2 and H2/H3 cross peaks in DQF-COSY reveals that residue **A** has small $J_{1,2}$ (≈ 3 Hz) and large $J_{2,3}$ (≈ 10 Hz) coupling constants. Further spin connectivity cannot be established from H3 in DQF-COSY. The absence of further spin connectivity in DQF-COSY can be the consequence of dispersive peak cancelation due to a small $J_{3,4}$ coupling constant, which is expected for a galactopyranose configuration. The NOESY spectrum (Fig. 3), however, shows that H3 gives a cross peak to a proton spin at 4.22 ppm, which in turn shows a strong cross peak to a resonance at 4.43 ppm, indicating that these resonances are H3, H5 and H4 of residue **A** with a galactopyranose configuration [23]. The assignments of H3, H4, and H5 were further confirmed in HMBC (Fig. 4) where the anomeric proton resonance gives long-range correlation to its C3 at 74.4 ppm and to C5 at 73.9 ppm. H3 and H5 chemical shifts are 4.16 ppm and 4.22 ppm respectively according to HMQC (Fig. 1). Further support for the spin connectivity
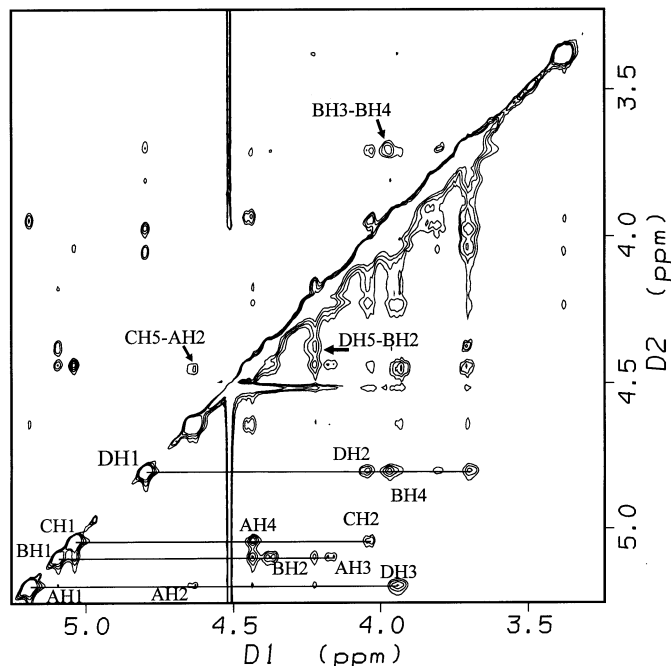
Fig. 3. Phase-sensitive NOESY spectrum with 60 ms mixing time of the polysaccharide from *V. vulnificus* 6353 at 500 MHz.

of residue **A** comes from the ring $^1H-^{13}C$ region in HMBC (Fig. 4c). In the HMBC spectrum, C3 and C5 show multiple bond correlation to H4. The strong NOESY cross peak between H1 and H2 (Fig. 3) confirms its α-configuration. The absence of an H6 signal in residue **A** suggests its identity as a uronic acid. LRHMQC with a 50-ms delay (Fig. 5b) correlates a carbonyl ^{13}C at 174.82 ppm with **A**-H5 at 4.22 ppm. The **A**-C2 chemical shift at 49.8 ppm suggests an acetamido function at position 2. Based on the above data, residue **A** is tentatively assigned as a 2-acetamido-2-deoxyhexuronate in the *α-galacto* configuration.

The anomeric proton of residue **B** at 5.09 ppm gives a cross peak to the H2 proton at 4.37 ppm, which further shows a cross peak to H3 at 3.70 ppm, in DQF-COSY (Fig. 2). While there is no further connectivity in DQF-COSY, NOESY data (Fig. 3) connect H3 to H4 at 3.97 ppm. Connection beyond H4 is most conveniently detected in the HMBC spectrum (Fig. 4a) which shows that H1 gives long-range intra-residue correlation to C3 and C5 typical of an α-pyranoside residue. The chemical shifts of H3 and H5 positions can be read from HMQC (Fig. 1). DQF-COSY connects H5 to both H6 and H6'. Small $J_{1,2}$ coupling (less than 3 Hz) and a NOESY cross peak between H1 and H2 implies that residue **B** is in the α-anomeric configuration. The ^{13}C chemical shift of C2 is 50.1 ppm, indicating that there is an acetamido group at position 2. Therefore, residue **B** is tentatively identified as α-*N*-acetylgalactosamine.

The anomeric proton H1 at 4.80 ppm of residue **D** gave a cross peak to H2 at 4.05 ppm and the remaining connectivity up to the methyl resonance at H6 can be detected in DQF-COSY and in HOHAHA. Because there is partial cancelation of central multiplets of the cross peaks in the DQF-COSY spectrum, proton homonuclear coupling constants were estimated from the HMQC spectrum. The pseudotriplet lineshapes of H3 (3.93 ppm) and H4 (3.38 ppm) in HMQC imply that $J_{2,3}$, $J_{3,4}$ and $J_{4,5}$ are approximately 10 Hz. As in residues **A** and **B**, H2 for this residue correlates with a carbon resonance at 53.9 ppm in the HMQC spectrum, implying the presence of an acetamido group at the C2 position. The α-anomeric configuration is shown

by the small $J_{1,2}$ coupling as well as a strong NOESY cross peak between H1 and H2 (Fig. 3). Thus, residue **D** is 2-acetamido-2,6-dideoxyglucopyranose (QuiNAc).

The anomeric resonance at 5.04 ppm for residue **C** shows a cross peak to H2 at 4.03 ppm, and the connectivity up to H5 can be traced out in DQF-COSY (Fig. 2). HOHAHA data also show the connectivity from H1 to H4 (data not shown). The lineshapes for both H3 and H4 appear as pseudotriplets in HMQC identifying a *gluco* configuration for residue **C**. The absence of an H6 proton suggests a carbonyl and in the LRHMQC spectrum (Fig. 5c) a carbonyl ^{13}C resonance at 173.30 ppm correlates with H5 at 4.44 ppm as well as H4 at 3.70 ppm indicating a uronic acid. The chemical shift of C2 at 54.7 ppm implies an acetamido sugar. The assignment of the α-anomeric configuration is based on the a strong NOESY cross peak between H1 and H2 (Fig. 3) and small J_{12} coupling constant from DQF-COSY. Thus, residue **C** is tentatively assigned as 2-acetamido-2-deoxy-α-glucuronic acid (GlcNAcA). In this residue, as well as all the other amino sugars in this polymer, LRHMQC shows correlation between carbonyl ^{13}C resonances and the methyl proton signals near 2.0 ppm confirming that all four amino sugars in the polymer are *N*-acetylated.

With the assignment of the proton signals described above, the ^{13}C signal assignment can be obtained by direct correlation to bonded protons in the HMQC spectrum (Fig. 1). This assignment, given in Table 1, accounts for all the signals of carbon-bound protons in the *V. vulnificus* 6353 polysaccharide. Correlation with a direct ^{13}C spectrum (not shown) indicates that six carbonyl ^{13}C signals can also be accounted for by this assignment. The homonuclear and heteronuclear NMR experiments suggest that the *V. vulnificus* 6353 polysaccharide consists of four repeating sugar residues α-QuiNAc, α-GalNAc, α-GalNAcA and α-GlcNAcA.

But this assignment of the constituent sugars was not complete as was shown by amide proton spectra. Signals of these exchangeable protons can be recorded in H_2O solution with suitable techniques for suppression of the water resonance which are well known in protein NMR spectroscopy. In the 2D amide proton HOHAHA spectrum, four signals due to secondary amides are detected each of which is coupled into the spin system of the four acetamido sugars as indicated in the data of Table 2. In addition, the amide proton spectra show two additional resonances which are coupled together but are not coupled to any of the carbon-bound protons of the sugar rings. This pattern is typical of primary amide proton signals such as those of asparagine side chains in proteins. In water-suppressed NOESY spectra, the four resonances assigned to the secondary amides of the 2-acetamido sugars each show cross peaks to H1, H2 or H3 of their own sugar ring in addition to a few cross peaks to neighboring residues. The resonances at 7.27 and 7.64 ppm, which we assign to a primary amide, show cross peaks to carbon-bound protons at 3.70 ppm, a chemical shift which could correspond either to H3 or H6 of residue **B** or to H4 of residue **C**. These data, combined with HPAEC data to be described below, suggest that the α-2-acetamido-2-deoxyglucuronic acid (GlcNAcA) residue is in fact a uronic acid amide. For a similar glucuronamide, Sadovskaya et al. [24] observed an NOE cross peak between the primary amide signals and H5 but such a cross peak could not be observed in our system due to the proximity of the **C** H5 resonance at 4.23 ppm to the water signal.

Monosaccharide composition analysis of the *V. vulnificus* 6353 polysaccharide with HPAEC shows two peaks at 7.23 ± 0.2 min and 11.28 ± 0.2 min with 15 mM NaOH as eluant. The peak eluting at 7.23 ± 0.2 min was identified as quinovosamine by comparing its retention time to that of standard quinovosamine identified in the capsular polysaccharide of *V.*
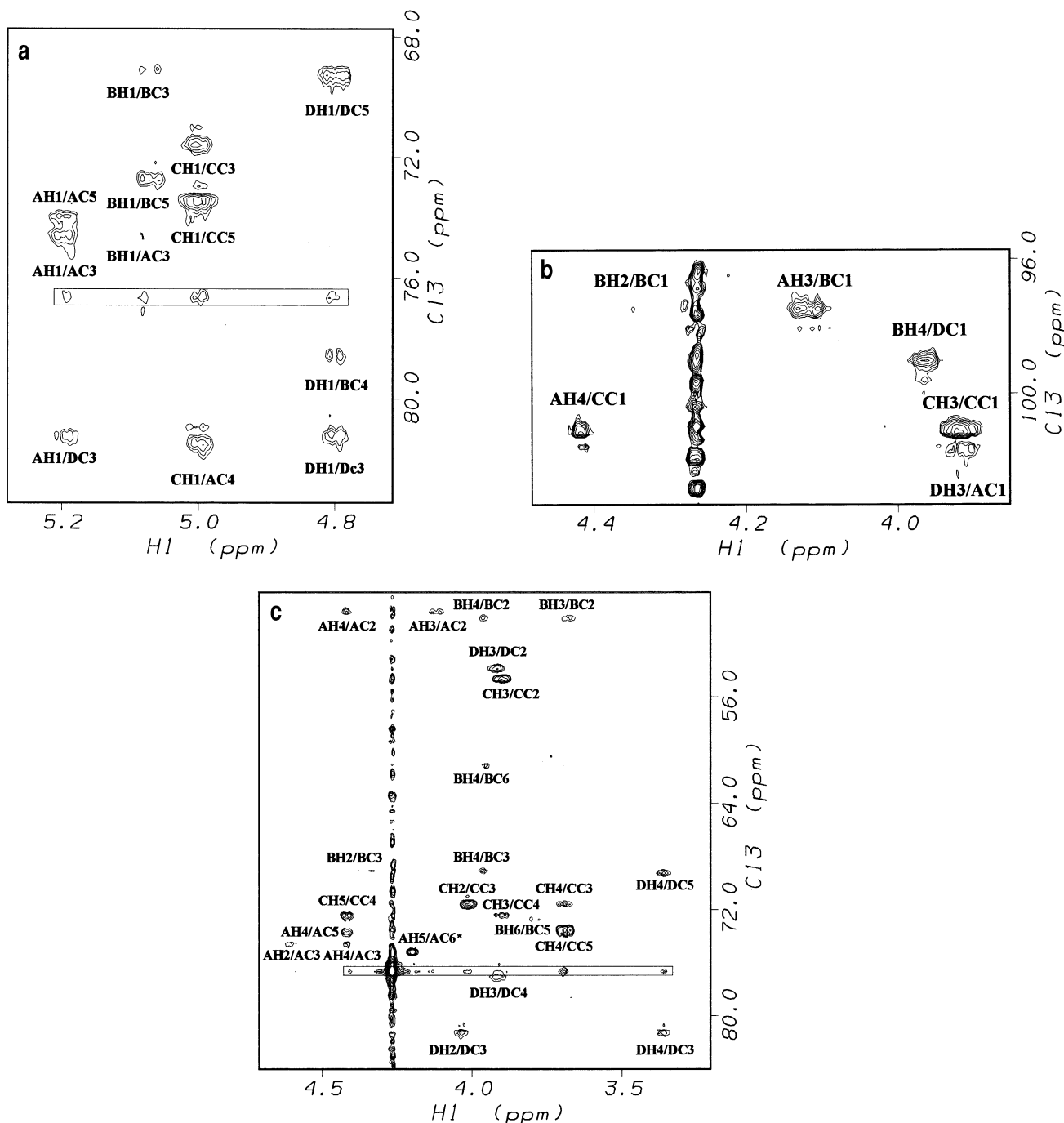
Fig. 4. ¹H-¹³C HMBC spectrum of *V. vulnificus* 6353 polysaccharide at 500 MHz. (a) Expansion of the anomeric proton region. (b) Expansion of the anomeric carbon region. (c) Expansion of the ring proton and carbon region. Peaks inside squares are artifacts at the ¹³C carrier frequency. Peak HA5/CA6 (asterisk) is a folded cross peak between H5 and carbonyl ¹³C of residue **A**.

vulnificus MO6-24/O [13]. The other peak at 11.23 ± 0.2 min exactly matched standard galactosamine. Under stronger chromatographic elution conditions (eluant 2) for identifying uronic acids, we observed peaks at 3.90 min, 5.63 min and 7.60 min as well as later-eluting peaks. The peak at 5.63 min coincides with aminogalacturonic acid and that at 7.60 min coincides with our synthetic sample of aminoglucuronic acid. The other peaks in the chromatogram may be di- and tri-saccharides resulting from incomplete cleavage of the linkages of the aminouronic acids by acid hydrolysis.

To provide an authentic sample of 2-amino-2-deoxyglucuronic acid for HPLC and to confirm its NMR properties, a syn-

thetic sample was prepared according to Heyns and Paulsen [15]. Its ¹H-NMR spectrum was conveniently assigned by means of a DQF-COSY spectrum (not shown) which showed approximately equal amounts of *α*- and *β*-anomers in equilibrium. ¹³C chemical shifts were assigned with data from the HMQC spectrum and chemical shifts were consistent with the corresponding residue in the *V. vulnificus* 6353 polysaccharide. Chemical shifts are reported in Table 3. LRHMQC data (not shown) indicated long-range correlation of the C6 carbonyl resonances at 176.9 ppm (*α*-) and 175.9 ppm (*β*-) to both H4 and H5 similar to that observed for GlcNAcA in the polysaccharide (Fig. 5).
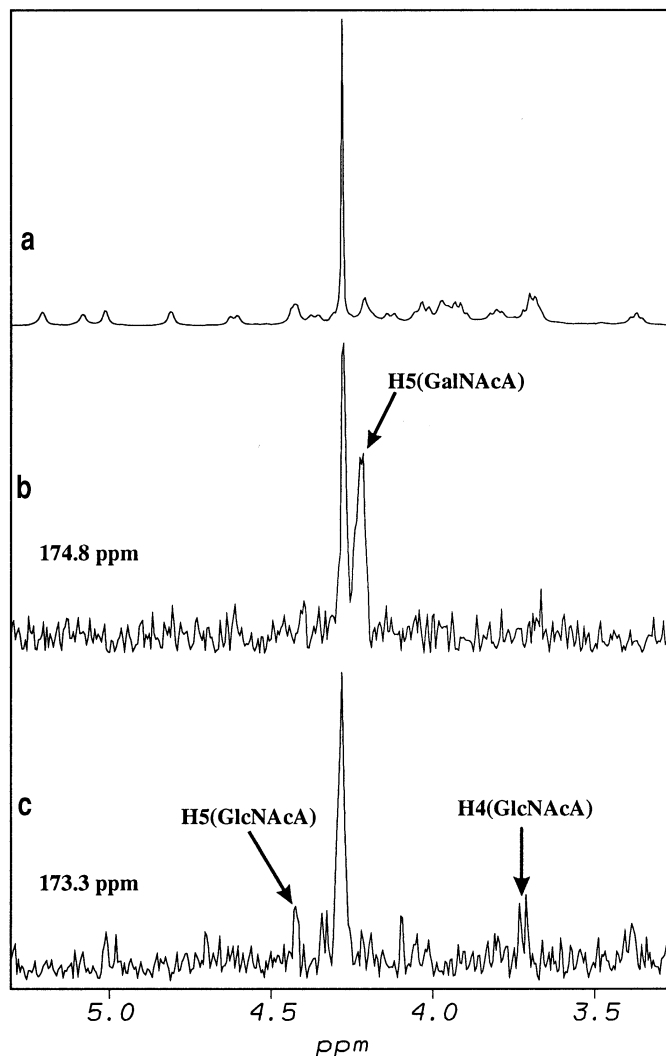
Fig. 5. ¹H-¹³C LRHMQC spectrum of *V. vulnificus* 6353 polysaccha-ride at 500 MHz at 75 °C. (a) Expansion of the downfield proton spectrum at 75 °C, (b) Expanded row vector at ¹³C chemical shift of 174.82 ppm, (c) Expanded row vector at ¹³C chemical shift of 173.30 ppm.

Table 1. NMR chemical shifts of *Vibrio vulnificus* 6353 polysaccha-ride in D₂O at 50 °C. ¹H-NMR chemical shifts are given with reference to internal 4,4-dimethyl-4-silapentane 1-sulfonate with acetone as the internal standard (2.225 ppm downfield). ¹³C chemical shifts are given with reference to internal acetone (31.07 ppm).

Atom		Chemical shift in residue			
		α-GalNAcA (A)	α-GalNAc (B)	α-GlcNAcANH₂ (C)	α-QuiNAc (D)
		ppm			
¹H	H1	5.19	5.09	5.04	4.80
	H2	4.64	4.37	4.03	4.05
	H3	4.16	3.70	3.92	3.93
	H4	4.43	3.97	3.70	3.38
	H5	4.22	3.98	4.44	4.23
	H6	–	3.81	–	1.23
	H6′	–	3.69	–	–
¹³C	C1	101.5	97.7	101.3	99.2
	C2	49.8	50.1	54.7	53.9
	C3	74.4	69.0	71.5	81.3
	C4	81.5	78.4	72.3	76.9
	C5	73.9	72.6	73.4	69.2
	C6	174.82	61.1	173.30	17.2

Table 2. Amide proton NOE data for *V. vulnificus* 6353 polysaccha-ride at 40 °C.

Residue	δ_{NH}	Major cross peaks				
	ppm					
GalNAcA−A	7.70	5.19 (s) A H1	3.97 (s) B H4	3.38 (w) D H4		
GalNAc−B	7.63	5.08 (w) B H1	5.04 (m) C H1	3.71 (s) B H6 B H3 C H4		
GlcNAcANH₂ C	7.33	5.04 (s) C H1	4.04 (s) C H2	3.93 (s) C H3		
QuiNAc D	8.47	5.19 (w) A H1	4.05 (s) D H2	3.93 (s) D H3	3.81 (m) B H6′	3.69 (w) B H6 B H3 C H4
Primary amide	7.27	7.67 (vs) primary amide	3.70 (m) B H6 B H3 C H4			
Primary amide	7.67	7.27 (vs) primary amide	3.70 (s) B H6 B H3 C H4			

We had expected carbohydrate analysis by HPAEC following reduction to show glucosamine resulting from reduc-tion of GlcNAcA. But these experiments were negative, in spite of repeated efforts to reduce the polysaccharide under conditions which have been routinely effective for reduction of amino uro-nic acids in other polysaccharides in our laboratory. These re-sults, when combined with the detection of a primary amide in the amide proton spectra, lead us to conclude that the GlcNAcA residue is, in fact, a uronic acid amide which is hydrolyzed to aminoglucuronic acid in the normal carbohydrate analysis proto-col.

Given the monosaccharide composition analysis together with the complete proton and carbon assignments, the glycosidic linkages of these residues in the polysaccharide can be estab-lished by the long-range ¹H−¹³C HMBC as shown in Fig. 4. All the anomeric protons give intra-residue long-range connectivit-ies to C3 and C5, consistent with the α-anomeric hexopyranoside configuration [17, 23]. These anomeric protons also give strong correlation to aglycone carbon atom resonances of linked resi-dues through $^3J_{CH}$ except for the weak cross peak between **B**H1 and **A**C3 (see Fig. 4a). The cross peaks between all the anom-eric carbons and respective aglycone protons of linked residues

further confirm the residue linkages as shown in Fig. 4b. Ac-cording to the HMBC spectrum, residue **B** (α-GalNAc) is linked to residue **A** (α-GalNAcA) through a (1→3)-linkage, residue **A** (α-GalNAcA) is linked to residue **D** (α-QuiNAc) through (1→3)-linkage and residue **D** (α-QuiNAc) is linked to **B** (α-Gal-NAc) through (1→4)-linkage. Therefore, residues **B** (α-Gal-NAc), **A** (α-GalNAcA) and **D** (α-QuiNAc) form the polymer backbone. Residue **C** (α-GlcNAcANH₂) is linked (1→4) to resi-due **A** (α-GalNAcA) to form a side chain. In addition to HMBC results, NOESY data (Fig. 3) show cross peaks across each of the linkages.

Table 3. NMR chemical shifts of α- and β-2-amino-2-deoxyglucuro-nic acid in D$_2$O at 25 °C. Shifts were measured as in Table 1.

Atom		Shift in	
		α-GlcNA	β-GlcNA
		ppm	
^{1}H	H1	5.456	4.939
	H2	3.334	3.049
	H3	3.916	3.704
	H4	3.567	3.585
	H5	4.157	3.789
^{13}C	C1	90.08	93.57
	C2	54.95	57.47
	C3	70.37	72.81
	C4	72.90	72.90
	C5	72.80	77.11
	C6	176.9	175.9

For determination of the absolute configuration of the sugar residues, the polysaccharide was treated with 4 M HCl in 2-butanol to form diastereomeric glycosides [14]. GC analysis of the trimethylsilyl derivatives showed peaks corresponding to D-galactosamine and to our synthetic standard of 2-amino-2-deoxy-D-glucuronic acid. Chromatograms were also compared with those made from the butanolysis products of the capsular polysaccharide of *V. vulnificus* MO6-24 which is known to contain 2-amino-2-deoxy-D-galacturonic acid and L-quinovosamine [25]. The GC results indicate that that both residues in the *V. vulnificus* 6353 polysaccharide have the D absolute configuration.

Since crystalline samples were not available for all the constituent sugars, there was some uncertainty in the interpretations of some of the gas chromatograms. In addition, our butanolysis protocol required unusually strong acid conditions (4 M HCl) to de-N-acetylate the sugars for comparison to standard 2-amino-2-deoxy-D-glucuronic acid. Therefore we carried out molecular modeling studies on the repeating subunit of the proposed structure for the capsular polysaccharide of *V. vulnificus* 6353 to predict NOESY patterns expected for different combinations of D and L residues [24, 26]. The data of Fig. 3 show strong cross peaks across the GalNAc α-(1→3)-GalNAcA linkage between **B** H1 and both **A** H3 and **A** H4. Our disaccharide model with both residues in the D configuration shows the distances between these protons to be 2.6 Å and 2.2 Å, respectively. Previous studies have shown that such cross peaks are especially diagnostic of sugar configuration for the case of an equatorial proton (**A** H4) adjacent to an equatorial glycosidic linkage [27]. Fig. 3 also shows a strong cross peak between **C** H5 and **A** H2 in a spectral region with few overlapping resonances. Our model for the disaccharide GlcNAcA α-(1→4)-GalNAcA shows these two protons to be 2.5 Å apart in the low-energy conformation of the diastereomer with both residues in the D configuration, while they are distant in the model with the two sugars in different absolute configurations. This argument that residues **C** and **A** have the same (D) absolute configuration can also be applied to residues **B** and **D** which also show a cross peak between **B** H2 and **D** H5. Thus, comparison of molecular modeling results with the NOESY data of Fig. 3 supports our conclusion that all the four sugar residues have the D configuration. A model of the tetrasaccharide repeating unit was constructed from the minimum energy disaccharide conformations and was further subjected to energy minimization which caused modest changes up to 20° in the glycosidic dihedral angles. In the minimized tetrasaccharide, the glycosidic dihedral angles, (Φ,Ψ), following the standard heavy atom convention recommended by IUPAC are for the linkage **B-A**, (68°, 140°), for **C-A**, (96°, −91°) and for **A-D**, (68°, −141°).

Based on the above NMR and chromatography evidence, we propose the following repeating unit as the structure of the polysaccharide from *Vibrio vulnificus* strain 6353:

<div align="center">

B   **A**   **D**

[→4)α-D-Gal*p*NAc(1→3)-α-D-Gal*p*NAcA(1→3)-α-D-Qui*p*NAc(1→]$_n$

α-D-Glc*p*NAcANH$_2$ (1→4)-↗

C
</div>

DISCUSSION

The cell-surface polysaccharides of vibrios have received increasing attention in recent years. The unusual chemical structures of these complex carbohydrates have presented problems for detailed structural studies but the introduction of more powerful chemical methods, improved chromatography of carbohydrates and instrumental methods of analysis such as mass spectrometry and NMR spectroscopy have made structural studies more practical. While most work has focused on the lipopolysac-

Table 4. Structures of the capsular polysaccharides of *V. vulnificus*.

Strain	Structure
MO6−24 [10]	[→3)α-L-Qui*p*NAc(1→3)-α-D-Gal*p*NAcA(1→3)-α-L-Qui*p*NAc(1→]$_n$ α-L-Qui*p*NAc(1→4)-↗
BO62316 [13]	[→3)α-D-Fuc*p*NAc(1→3)-α-D-Gal*p*NAcA(1→3)-α-L-Qui*p*NAc(1→]$_n$ α-LRha*p*NAc(1→4)-↗
ATCC27562 [30]	serine NH-amide 6↗ [α-D-Glc*p*NAc(1→4)-α-D-Gal*p*A(1→4)-β-L-Rha*p*(1→4)-]$_n$ α-MurNAc(1→3)-↗

charides of vibrios, recent reports on *V. cholerae* O-139 Bengal, a cholera-causing strain indicate that, in contrast to the classical O-1 serotype, it is encapsulated. Its capsular polysaccharide, which is an important antigenic determinant, may become useful in vaccine development. The repeating subunit of this polysaccharide is comprised of six residues and contains β-D-QuiNAc, β-D-GlcNAc, α-D-GalA, a 4,6-cyclic phosphate of β-D-galactopyranose and two residues of α-colitose, a 3,6-dideoxy-hexose which is the L isomer corresponding to abequose [28, 29].

V. vulnificus has been of particular interest to us because of its striking virulence; persons who eat oysters containing the organism may become septic and die in intractable shock within $48-72$ h [1, 3]. There are preliminary data suggesting that the clinical effects are mediated, at least in part, by tumor necrosis factor α and that the capsular polysaccharide plays a role in stimulation of release of this factor [7]. Thus it would be valuable to identify a specific epitope on the capsular polysaccharides responsible for this effect of virulent strains of *V. vulnificus*. The molecular structure of such an epitope could be used as a starting point for design of therapeutic agents to inhibit the toxic response to the organism. In an attempt to identify structural features common to the capsules of virulent strains, our group has reported, in addition to the polysaccharide from strain 6353, detailed structures from three other *V. vulnificus* strains isolated from patients with septicemia [12, 13, 30]. While the absolute configurations of the monosaccharides of strains MO-6/24 [12] and BO62316 [13] were not reported in the original structure papers, they have been determined subsequently by circular dichroic methods [25, 31, 32]. The absolute configurations included in the summary of Table 4 are consistent with the NOESY spectra in the original papers [12, 13]. Each structure is rich in *N*-acetyl amino sugars and has a pattern of four monosaccharides in the repeating unit with three sugars in the backbone and a single side chain attached to a uronic acid residue in the D-*galacto* configuration. Note that the polysaccharides of both strains MO6/24 and BO-2316 are all $(1{\rightarrow}3)$-linked in the backbone while strains 6353 and ATCC 27562 have $(1{\rightarrow}4)$ linkages. While there are a few similarities, superficial examination of the chemical structures reveals no obvious common epitope. More detailed molecular modeling studies might reveal some common three-dimensional features.

Although it appears that the presence of capsule is strongly correlated with pathogenicity, we and others have shown by both immunological methods as well as by chemotyping by carbohydrate chromatography that there is a wide variety of capsular types associated with pathogenic *V. vulnificus* [10, 11, 33]. While a broad survey profiling the carbohydrate composition of capsular polysaccharides of strains isolated environmental sources revealed a remarkable variety of different capsular structures, it did not reveal striking differences in carbohydrate composition between pathogenic and environmental strains [11].

Vibrio polysaccharides contain a number of rare amino sugars not commonly found in lipopolysaccharides or capsules. *V. vulnificus* ATCC 27562 contains muramic acid, commonly found only in peptidoglycan. Its diastereomer, isomuramic acid has been found in the O-chain of some lipopolysacharides [30]. Likewise, the finding of 2-acetamido-2-deoxy-D-glucuronamide in strain 6353 is somewhat unusual. A similar primary amide of 2,3-diamino-2,3-dideoxy-glucuronic acid has been reported in both the O-anitgen and in the capsular polysaccharide of *V. anguillarum* serotype O:2 [24]. Although GlcNA has been known for some time [15], it appears that this monosaccharide has been found in few natural sources. It was reported as a component of a polysaccharide antigen from *Staphylococcus aureus* in which it occurs as a β-D-pyranosyl residue [34]. Aminoglucuronic acid was later reported to be a component of an acidic

capsular polysaccharide from *Achromobacter georgiopolitanum* [35]. More recently it has been found in the extracellular polysaccharides of certain black yeasts, *Rhinocladiella elatior* and *Rhinocladiella mansonii* [36]. Within the last decade, technical advances have facilitated complete structure determinations for many bacterial polysaccharides yet it is somewhat remarkable that this monosaccharide has not been documented in any of these recently reported structures.

REFERENCES

1. Blake, P. A., Merson, M. M., Weaver, R. E., Hollis, D. B. & Heublein, P. C. (1979) Disease caused by a marine vibrio: clinical characteristics and epidemiology, *N. Engl. J. Med. 300*, 1−5.
2. Morris, J. G. & Black, R. E. (1985) Cholera and other vibrios in the United States, *N. Engl. J. Med. 312*, 343−350.
3. Klontz, K. C., Leib, S., Schreiber, M., Janowski, H. T., Baldy, L. M. & Gunn, R. A. (1988) Syndromes of *Vibrio vulnificus* infections; clinical and epidemelogic features in Florida cases, *Ann. Int. Med. 109*, 318−323.
4. Kaysner, C. A., Abeyta, C., Wekell, M. M., DePaola, A., Stott, R. F. & Leitch, J. M. (1987) Virulent strains of *Vibrio vulnificus* isolated from estuaries of the United States West coast, *Appl. Environ. Microbiol. 53*, 1349−1351.
5. Wright, A. C., Hill, R. T., Johnson, J. A., Roghman, M. C., Colwell, R. R. & Morris, J. G. (1996) Distribution of *Vibrio vulnificus* in the Chesapeake Bay, *Appl. Environ. Microbiol. 62*, 717−724.
6. Wright, A. C., Simpson, L. M., Oliver, J. D. & Morris, J. G. (1990) Phenotypic evaluation of acapsular transposon mutants of *Vibrio vulnificus*, *Infect. Immun. 58*, 1769−1773.
7. Powell, J. L., Wright, A. C., Wasserman, S. S., Hone, D. M. & Morris, J. G. (1997) Release of tumor necrosis factor α in response to *Vibrio vulnificus* capsular polysaccharide in *in vivo* and *in vitro* models, *Infect. Immun. 65*, 3713−3718.
8. Devi, S. J. N., Hayat, U., Frasch, C. E., Kreger, A. S. & Morris, J. G. (1995) Capsular polysaccharide-protein conjugate vaccines of carbotype 1 *Vibrio vulnificus* − construction, immunogenicity, and protective efficacy in a murine model, *Infect. Immun. 63*, 2906−2911.
9. Devi, S. J. N., Hayat, U., Powell, J. & Morris, J. G. (1996) Preclinical immunoprophylactic and immunotherapeutic efficacy of antisera to capsular polysaccharide-tetanus toxoid conjugate vaccines of *Vibrio vulnificus*, *Infect. Immun. 64*, 2220−2224.
10. Hayat, U., Reddy, G. P., Bush, C. A., Johnson, J. A., Wright, A. C. & Morris, J. G. (1993) Capsular types of *Vibrio vulnificus*: An analysis of strains from clinical and environmental sources, *J. Infect. Dis. 168*, 758−762.
11. Bush, C. A., Patel, P., Gunawardena, S., Powell, J., Joseph, A., Johnson, J. A. & Morris, J. G. (1997) Classification of *Vibrio vulnificus* strains by the carbohydrate composition of their capsular polysaccharides, *Anal. Biochem. 250*, 186−195.
12. Reddy, G. P., Hayat, U., Abeygunawardana, C., Fox, C., Wright, A. C. Maneval, D. R., Bush, C. A. & Morris, J. G. (1992) Purification and structure determination of *Vibrio vulnificus* capsular polysaccharide, *J. Bacteriol. 174*, 2620−2630.
13. Reddy, G. P., Hayat, U., Bush, C. A. & Morris, J. G. (1993) Capsular polysaccharide structure of a clinical isolate of *Vibrio vulnificus* strain BO-62316 determined by heteronuclear nmr spectroscopy and high-performance anion-exchange chromatography, *Anal. Biochem. 214*, 106−115.
14. Gerwig, G. J., Kamerling, J. P. & Vliegenthart, J. F. G. (1979) Determination of the absolute configuration of monosaccharides in complex carbohydrates by capillary g.l.c., *Carbohydr. Res. 77*, 1−7.
15. Heyns, K. & Paulsen, H. (1955) Synthese der D-Glucosamineuronsäure (2-amino-2-desoxy-D-Glucuronsäure) und einiger ihrer Derivate, *Chem. Ber. 88*, 188−195.

16. States, D. J., Haberkorn, R. A. & Ruben, D. J. (1982) A two-dimensional nuclear Overhauser experiment with pure absorption phase in four quadrants, *J. Magn. Reson. 48*, 286−292.

17. Abeygunawardana, C., Bush, C. A. & Cisar, J. O. (1990) The complete structure of the polysaccharide from *Streptococcus sanguis* J22, *Biochemistry 29*, 234−248.

18. Bax, A., Griffey, R. H. & Hawkins, B. L. (1983) Correlation of proton and nitrogen-15 chemical shifts by multiple quantum NMR, *J. Magn. Reson. 55*, 301−315.

19. Shaka, A. J., Keeler, J. & Freeman, R. (1983) Evaluation of a new broadband decoupling sequence: waltz-16, *J. Magn. Reson. 53*, 313−340.

20. Bax, A. & Summers, M. F. (1986) H1 and C13 assignments from sensitivity-enhanced detection of heteronuclear multiple-bond connectivity by 2D multiple quantum NMR, *J. Am. Chem. Soc. 108*, 2093−2094.

21. Hore, P. J. (1983) Solvent suppression in fourier transform nuclear magnetic resonance, *J. Magn. Reson. 55*, 283−300.

22. Ha, S. N., Giammona, A., Field, M. & Brady, J. W. (1988) A revised potential-energy surface for molecular mechanics studies of carbohydrates, *Carbohydr. Res. 180*, 207−221.

23. Abeygunawardana, C. & Bush, C. A. (1993) Determination of the chemical structure of complex polysaccharides by heteronuclear NMR spectroscopy, *Adv. Biophys. Chem. 3*, 199−249.

24. Sadovskaya, I., Brisson, J. R., Altman, E. & Mutharia, L. M. (1996) Structural studies of the lipopolysaccharide O-antigen and capsular polysaccharide of *Vibrio anguillarum* serotype O:2, *Carbohydr. Res. 283*, 111−127.

25. Chang, C.-C. (1992) Determination of the absolute configuration of the sugar residues of polysaccharides by circular dichroism spectroscopy, Thesis, University of Maryland Baltimore County.

26. Kulakowska, M., Brisson, J. R., Griffith, D. W., Young, N. M. & Jennings, H. J. (1993) High-resolution nmr spectroscopic analysis of the C-polysaccharide of *Streptococcus pneumoniae*, *Can. J. Chem. 71*, 644−648.

27. Lipkind, G. M., Shashkov, A. S., Mamyan, S. & Kochetkov, N. K. (1988) The nuclear Overhauser effect and structural factors determining the conformations of disaccharide glycosides, *Carbohydr. Res. 181*, 1−12.

28. Preston, L. M., Xu, Q., Johnson, J. A., Joseph, J., Maneval, D. R., Husain, K., Reddy, G. P., Bush, C. A. & Morris, J. G. (1995) Preliminary structure determination of the capsular polysaccharide of *Vibrio cholerae* O139 Bengal AI1837, *J. Bacteriol. 177*, 835−838.

29. Knirel, Y. A., Paredes, L., Jansson, P. E., Weintraub, A., Widmalm, G. & Albert, M. J. (1995) Structure of the capsular polysaccharide of *Vibrio cholerae* O139 synonym Bengal containing D-galactose 4,6-cyclophosphate, *Eur. J. Biochem. 232*, 391−396.

30. Gunawardena, S., Reddy, G. P., Wang, Y., Kolli, V. S. K., Orlando, R., Morris, J. G. & Bush, C. A. (1998) Structure of a muramic acid containing capsular polysaccharide from the pathogenic strain of *Vibrio vulnificus* ATCC 27562, *Carbohydr. Res.*, in the press.

31. Mirle, A. R. (1994) Circular dichroism methods for the determination of the absolute configuration of monosaccharides derived from bacterial polysaccharides, Thesis, University of Maryland Baltimore County.

32. Kaluarachchi, K. & Bush, C. A. (1989) Determination of the absolute configuration of the sugar residues of complex polysaccharides by circular dichroism spectroscopy, *Anal. Biochem. 179*, 209−215.

33. Simonson, J. G. & Siebeling, R. J. (1993) Immunogenicity of *Vibrio vulnificus* capsular polysaccharides and polysaccharide-protein conjugates, *Infect. Immun. 61*, 2053−2058.

34. Hanessian, S. & Haskell, T. H. (1964) Structural studies of staphylococcal polysaccharide antigen, *J. Biol. Chem. 239*, 2758−2764.

35. Smith, E. J. (1968) Purification and properties of an acidic polysaccharide isolated from *Achromobacter georgiopolitanum*, *J. Biol. Chem. 243*, 5139−5144.

36. Kenne, L., Lindberg, B., Petersson, K. & Unger, P. (1980) Structural studies of the extracellular polysaccharides elaborated by *Rhinocladiella elatior* and *Rhinocladiella mansonii*, *Carbohydr. Res. 84*, 184−186.